AIP | The Journal of Chemical Physics

A theoretical simulation of the resonant Raman spectroscopy of the H2O···Cl2 and H2O···Br2 halogen-bonded complexes

Ricardo Franklin-Mergarejo, Jesús Rubayo-Soneira, Nadine Halberstadt, Kenneth C. Janda, and V. Ara Apkarian

Citation: The Journal of Chemical Physics **144**, 054307 (2016); doi: 10.1063/1.4940778
View online: http://dx.doi.org/10.1063/1.4940778
View Table of Contents: http://scitation.aip.org/content/aip/journal/jcp/144/5?ver=pdfcov
Published by the AIP Publishing

A theoretical simulation of the resonant Raman spectroscopy of the $H_2O\cdots Cl_2$ and $H_2O\cdots Br_2$ halogen-bonded complexes

Ricardo Franklin-Mergarejo,[1,2,3,a)] Jesús Rubayo-Soneira,[3] Nadine Halberstadt,[1,2,b)] Kenneth C. Janda,[4] and V. Ara Apkarian[4]
[1]*Université de Toulouse, UPS, Laboratoire Collisions Agrégats Réactivité, IRSAMC, F-31062 Toulouse, France*
[2]*CNRS, UMR 5589, F-31062 Toulouse, France*
[3]*InSTEC, Quinta de los Molinos, Ave. Salvador Allende y Luaces, Plaza, Ciudad Habana, Cuba*
[4]*Department of Chemistry, University of California, Irvine, Irvine, California 92697-2025, USA*

(Received 14 November 2015; accepted 14 January 2016; published online 4 February 2016)

The resonant Raman spectra of the $H_2O\cdots Cl_2$ and $H_2O\cdots Br_2$ halogen-bonded complexes have been studied in the framework of a 2-dimensional model previously used in the simulation of their UV-visible absorption spectra using time-dependent techniques. In addition to the vibrational progression along the dihalogen mode, a progression is observed along the intermolecular mode and its combination with the intramolecular one. The relative intensity of the inter to intramolecular vibrational progressions is about 15% for $H_2O\cdots Cl_2$ and 33% for $H_2O\cdots Br_2$. These results make resonant Raman spectra a potential tool for detecting the presence of halogen bonded complexes in condensed phase media such as clathrates and ice. © *2016 AIP Publishing LLC.* [http://dx.doi.org/10.1063/1.4940778]

I. INTRODUCTION

A number of experiments are using molecular halogens as reporters of local structure and dynamics to investigate their various water environments: ice,[1,2] clathrate hydrates,[2–6] and liquid water.[2,6] The spectroscopy of these molecules in the gas phase is well known, both in the infrared and visible-near UV regions. Interactions with their environment can thus be detected through changes in their spectra. The nature and importance of these changes is directly related to the importance and nature of these interactions.

Guest molecules of typical clathrate hydrates are usually located near the center of the clathrate cages, with non-specific interactions with the water molecules of the cage walls. However, infrared spectroscopy and accompanying molecular dynamics studies[7] have shown that in the case of molecules that are capable of strong to intermediate H-bonding to water, such as small ethers and H_2S, there can be an important proportion of point defects in the host lattice due to defect stabilization by hydrogen bond formation between the guest molecules and water molecules from the cage walls. This was confirmed by later studies on clathrate hydrates with small-cage guests capable of binding to the oxygen sites of the water lattice and hydrogen acceptors such as tetrahydrofuran or trimethylene oxide as large-cage guests.[8] Cooling of these clathrate hydrates showed that they converted to altered structures in which most guest molecules establish hydrogen bonds to water. This was achieved through configurations in which a large-cage guest accepted a proton and a small-cage guest donated a proton to a common water molecule of the shared wall. These unusual clathrate structures were named "nonclassical" in contrast with the usual, "classical" structures which involved only nonspecific (van der Waals) guest-lattice interactions.

Water-halogen interactions do not involve hydrogen bonding. However, the corresponding binding energies are significantly larger than the ones involved in usual van der Waals bonds (D_e = 982 cm^{-1} for $H_2O\cdots Cl_2$, 1273 cm^{-1} for $H_2O\cdots Br_2$, from Ref. 9). This is due to the strong interaction between the electrons from one of the oxygen lone pair orbitals and the empty σ^* orbital of the halogen molecules which is pointing outward along the dihalogen axis. This makes the oxygen and the two halogen atoms collinear, as established by microwave[10,11] and infrared spectroscopies[12–14] and confirmed by *ab initio* calculations.[9–11,14–16] Using the analogy with the (stronger) hydrogen bond, this specific bonding has been called "halogen bond." Hence, there is a strong incentive to detect the possible formation of these one-to-one complexes in clathrates or in other condensed water environments. In particular for clathrates the possible existence of lattice defects could be stabilized by forming halogen bonds. Experimental and theoretical investigations have been conducted in order to characterize the nature of halogen-water interactions in clathrate hydrates, ice, and liquid water. They are summarized below. Here, we study the resonant Raman (RR) spectra of $H_2O\cdots Cl_2$ and $H_2O\cdots Br_2$ and show that the existence of these halogen-bonded complexes should be characterized by the presence of an intermolecular water-halogen stretching vibration.

Raman spectra recorded for Cl_2, Br_2, and BrCl clathrate hydrates[17] revealed remarkably weak interaction between the Cl_2 or Br_2 molecule and its water environment, slightly more for BrCl, based on the small change in vibrational frequency. Interestingly, one low frequency band was detected for each

a)Current address: Universidad Nacional de Quilmes, Roque Saenz Pea 352, B1876BXD Bernal, Argentina. Electronic mail: rfmergarejo@gmail.com
b)Nadine.Halberstadt@irsamc.ups-tlse.fr

clathrate, at 103, 130, and 88 cm^{-1} for Cl_2, Br_2, and BrCl, respectively. These low frequency bands were tentatively assigned to translational vibrations of the water lattice. Note that these were non-resonant Raman spectra, and hence the intensity of intermolecular vibrations from possibly existing water-halogen complexes could be different.

UV-visible spectroscopy has been used by Kerenskaya *et al.*[2] to study bromine molecules confined in clathrate hydrate cages. These authors showed that the absorption bands were shifted to the blue, while retaining the spectral envelope of gas phase spectra. This was in contrast to spectra of bromine in liquid water or amorphous ice which were broadened and significantly more blue-shifted. The blue shift varied from about 360 cm^{-1} in large $5^{12}6^4$ cages of type II clathrates and about 900 cm^{-1} in pure bromine hydrate clathrates with a combination of $5^{12}6^2$ and $5^{12}6^3$ cages, to more than 1700 cm^{-1} in liquid water and amorphous ice.

The same differences were found for iodine molecules trapped in sII clathrate hydrate structures stabilized by tetrahydrofuran (THF), CH_2Cl_2, or $CHCl_3$.[3] The UV-visible absorption spectrum of I_2 exhibited a relatively large blue shift, of the order of 1440 cm^{-1}, in clathrates, while its spectrum in water and in ice was dramatically broadened and blue-shifted by about 3000 cm^{-1}.

Chlorine clathrate hydrate absorption spectra were recorded at 200 K and 77 K in conditions where chlorine is located in the larger $5^{12}6^2$ cages, and showed a surprising temperature dependence.[5] At 200 K, the spectrum was very similar to that of gas phase chlorine, while at 77 K, it was shifted nearly as much as for aqueous chlorine solutions, but remained narrower than the aqueous spectrum. It was speculated that this strong blue shift was due to chlorine molecules settling into a fixed position near the cage walls.

Resonant Raman was also used to probe the I_2 environment. A vibrational progression up to $v = 6$ was observed in THF clathrate hydrate with a vibrational frequency equal to that of the free molecule. In contrast, in liquid water and in ice, the resonance Raman scattering was efficiently quenched. Resonant Raman also confirmed the existence of polymorphism in Br_2 clathrate hydrates,[4] thanks to the detection of long vibrational progressions. The vibrational parameters extracted from these progressions were $\omega_e = 321.2 \pm 0.1$ cm^{-1} and $\omega_e\chi_e = 0.82 \pm 0.05$ cm^{-1} in the TS-I structure determined by Udachin *et al.*,[18] and $\omega_e = 317.5 \pm 0.1$ cm^{-1} and $\omega_e\chi_e = 0.70 \pm 0.1$ cm^{-1} in the newly discovered structure assigned to CSII. This is still close to the gas phase values $\omega_e = 325.321$ cm^{-1} and $\omega_e\chi_e = 1.0774$ cm^{-1}. As first noticed by Fleyfel and Devlin,[19] molecules in larger cages tend to have lower vibrational frequencies.

All these spectroscopic data point to a weak interaction of the halogen molecule with a clathrate environment, somewhat similar to what was observed in rare gas matrices, and a stronger interaction in ice and much stronger interaction in liquid water. This is confirmed by dynamics studies using excitation to the first valence electronic states of halogen molecules. Since these states are repulsive in the Franck Condon region, excitation induces dissociation, which is followed by recombination when the departing atoms hit the cage walls of the host.[20]

Vibronic dynamics of I_2 trapped in amorphous ice has been studied by four-wave mixing experiments.[21] Two distinct dynamical behaviors were observed, leading to the conclusion that iodine molecules were trapped in two distinct types of sites. The first type was ascribed to asymmetric polar cages in which the absorption shift was as strong as in water, 3500 cm^{-1}, and vibronic transfer from the B to the ground electronic state was completed upon the first extension of the molecular bond. The iodine molecule was believed to be oxygen bonded to one water molecule on one side and hydrogen bonded to another one on the other side. The second type of sites exhibited coherent vibrational dynamics remaining in the B state, which suggested a cancellation of vibronic couplings due to a symmetric environment. The vibrational period of the wave packet evolved from 245 fs to 325 fs in the course of five oscillations, indicating adiabatic following of the cage expansion. In addition, the blue shift in the absorption spectrum was equal to that of iodine clathrate hydrates. It was concluded that this second ensemble of iodine molecules experienced a local symmetric water environment similar to that in a clathrate cage.

Transient grating measurements on bromine in single crystal clathrate hydrates and in aqueous solution have been used to study the dynamics induced by excitation to the B electronic state.[6] This was followed by cage-induced recombination to the A/A' states. In liquid water, recombination was incoherent and peaked at 1 ps, with a vibrational decay constant of 1.8 ps. In the tetragonal TS-I crystals with the smaller cages, recombination was faster, $t = 360$ fs, with a bond oscillation period of 240 fs, while in the CS-II crystals, recombination was slower, $t = 490$ fs, with a vibrational period of 290 fs and a shorter overall coherence time due to the larger cages and the looser fit around bromine. Analysis of the recombination time-distributions concluded that the effective liquid phase hydration shell was larger than that in a hydrate phase, structurally disordered, and anelastic. In ice, at 120 K, the enclathrated bromine population is observed to undergo fully coherent vibrational dissipation on the electronically excited B state.[22] Spectral decomposition of the data unravels a weak coupling to a lattice mode and its overtone, at ~40 and 80 cm^{-1}, which is ascribed to the clathrate cage breathing mode.

Resonant Raman also explores excited state dynamics. The incoming photon creates a wave packet in the resonantly excited electronic state, and the projection of the evolving wave packet on ground state vibrational wave functions determines the vibrational intensities in the RR spectrum. If the excited state is repulsive, and if no other decay process occurs, this wave packet propagates along the dissociation coordinate up to complete dissociation and all the vibrational levels of the ground state appear in the RR spectrum with intensity determined by the coordinate-dependent transition moment, and the dwell time of the wave packet on turning points of the ground state potential. In the other extreme, if electronic dephasing sets in before the excited state wave packet has had time to move, only the fundamental will be observed. Since dissociation corresponds to atomic displacements of the order of several Angströms, the dynamics that defines the RR spectrum is completed on a time scale of the order of femtoseconds.[23]

For halogen molecules, the B and C valence electronic states are repulsive in the Franck-Condon region, and therefore good candidates for RR studies in condensed water. Branigan *et al.*[24] recently studied liquid bromine, and Br_2 dissolved in water, via RR spectroscopy. They showed that resonant Raman scattering of Br_2 over the $B(^3\Pi_{0u}^+) \leftarrow X(^1\Sigma_g^+)$ transition is quenched in water, in contrast with liquid bromine where a progression of more than 35 overtones is observed.[25] Using a simple, semi-quantitative model, it was concluded that the hydration shell of bromine in water consisted of dynamically equivalent fluxional water molecules.

All the results obtained so far, both from the spectroscopic and the dynamical point of view, are compatible with the following microscopic picture. Dihalogen molecules in clathrates behave somewhat like dihalogen molecules in rare gas matrices, with a weak molecule-host interaction. This is ascribed to the fact that all the hydrogen bonds available from water molecules were used in building the clathrate cages. Hence, no oxygen lone pair electronic orbital would be available to form a specific halogen bond with a guest molecule. These "classical" structures[8] were confirmed by theoretical studies. Theoretical simulations of Cl_2 in 5^{12} and $5^{12}6^2$ cages,[26] Br_2 in clathrate hydrates,[27] and Br_2 in a $5^{12}6^2$ cage[28] have found the halogen molecules near the cage center, with no halogen bonding to a water molecule. In the other extreme, in aqueous solution, water-water hydrogen bonds are constantly forming and breaking, so that there is always the possibility to form a halogen bond between a halogen molecule and a water molecule in its hydration shell. These bonds are also constantly forming and breaking, and the result is a broad, strongly shifted absorption spectrum. In ice, the situation can be similar to that of water or to that of clathrate depending on the trapping site.

However, a recent study by Udachin *et al.* gave results that seem to contradict this overall picture. These authors have conducted X-ray crystallography experiments to determine the pure Cl_2 and Br_2, and mixed Cl_2–Br_2 clathrate structures.[29] They observed $O\cdots Cl$ and $O\cdots Br$ contact distances that were significantly shorter than the sum of their van der Waals radii. They concluded that this was evidence for halogen bonding between the water oxygen atoms and the dihalogen guests. This was quite unexpected since it was commonly believed that halogen bonding was not strong enough to disrupt the hydrogen bond network of the clathrate structure.

One convenient way to solve this controversy and detect the presence of these 1:1 water:halogen complexes in condensed phase is RR spectroscopy. Hence, it is important to characterize their RR spectra, and, in particular, to predict whether the intermolecular vibrations will be visible in addition to the dihalogen stretching lines. Observation of these intermolecular vibrations would then be a confirmation of the existence of these water-dihalogen complexes.

In the present paper, we report the results of RR spectral simulations for the $H_2O\cdots Br_2$ and $H_2O\cdots Cl_2$ binary complexes. Section II presents the time-dependent formalism used, based on the so-called Raman wave function,[30,31] the reduced dimensional model, and the corresponding potential energy surfaces (PESs) as well as the bound states. Section III shows the resulting RR spectra for the Cl_2 and Br_2 molecules, then for the $H_2O\cdots Cl_2$ and $H_2O\cdots Br_2$ complexes, followed by a discussion in Section IV. Section V is the conclusion of this study.

II. METHODOLOGY

A. Raman spectrum calculation: Raman wave function

In this work, we use the time-dependent formalism to determine the resonant Raman spectrum of $H_2O\cdots X_2$ complexes (X ≡ Cl or Br).[30–34] Within this framework, the RR scattering intensity $I_{f\leftarrow i}(\omega_I,\omega_S)$ for a transition from the initial vibrational level $|g,v_i\rangle$ to a final vibrational level $|g,v_f\rangle$ of the ground electronic state g is given by

$$I_{f\leftarrow i}(\omega_I,\omega_S) \propto \omega_I\omega_S^3|\alpha_{f\leftarrow i}(\omega_I)|^2$$

with

$$\alpha_{f\leftarrow i}(\omega_I) = \langle g,v_f|\mu_\lambda^{ge}|R(\omega_I)\rangle, \tag{1}$$

where $\hbar\omega_I$ and $\hbar\omega_S$ are the energy of the incident and scattered photon, respectively, $\boldsymbol{\mu}^{ge}$ is the transition dipole moment between the ground and resonantly excited electronic states, and μ_λ^{ge} its (tensor) component λ along the polarization axis. Finally, $R(\omega_I)$ is the so-called Raman wave function defined as[31]

$$|R(\omega_I)\rangle \equiv \int_0^{t_\infty} \exp\left(-i(H_e-\widetilde{E}_i)t/\hbar - \frac{t}{\tau_e}\right)\mu_\lambda^{eg}|g,v_i\rangle dt, \tag{2}$$

where $E_i = \langle g,v_i|H_g|g,v_i\rangle$ is the energy of the initial vibrational level $|g,v_i\rangle$ and $\widetilde{E}_i = \langle g,v_i|H_g|g,v_i\rangle + \hbar\omega_I$, H_g (H_e) is the molecular hamiltonian in the ground (excited) electronic state, and τ_e is a phenomenological electronic dephasing lifetime for the excited state e. The stationary Raman wave function, obtained by time integrating the excited state wave packet, contains all of the information necessary to reconstruct intensities of RR lines via the dipole-dressed overlap integrals in (1). The associated transition energies are given by the energy conservation condition for resonant Raman,

$$E_i + \hbar\omega_I = E_f + \hbar\omega_S, \tag{3}$$

where $E_f = \langle g,v_f|H_g|g,v_f\rangle$ is the energy of the final vibrational level $|g,v_f\rangle$.

The evaluation of Eq. (1) requires knowledge of the bound vibrational levels of the ground electronic state. As will be shown in the following, $R(\omega_I)$ involves a large range of excitations in both the halogen and the intermolecular coordinates and the *ab initio* potential energy surface available[9] did not extend far enough to describe the higher ones properly. However, we are mostly interested in the intensity ratios between intramolecular (X–X) and intermolecular (H_2O–X_2) vibrations. Hence, we focus on the lowest vibrational levels, for which the vibrational wave function can be determined with the available *ab initio* points.

B. Potential energy surface, transition dipole moment

As in previous work on the water-dihalogen absorption spectra,[9,35,36] we use here a reduced-dimension model for the

water-dihalogen complexes, which takes into account the two most relevant coordinates: the interhalogen distance denoted here as Q and the center of mass distance between the water and halogen molecules denoted as q.

The X and C *ab initio* PESs are taken from Ref. 9. They were determined on a grid 1.85 Å ≤ Q ≤ 2.25 Å and 3.6 Å ≤ q ≤ 12.00 Å for $H_2O\cdots Cl_2$, 1.80 Å ≤ Q ≤ 2.90 Å and 3.40 Å ≤ q ≤ 10.00 Å for $H_2O\cdots Br_2$. This grid is interpolated to 256×512 (Q,q) points using the 2-dimensional (2D) cubic spline technique.[37] The transition dipole moment was taken as a constant, which was a good approximation in the Franck-Condon region.[36] Its dependence on both Q and q coordinates is somewhat stronger at shorter distances. This could affect somewhat the intensity of higher vibrational states. However, this should not affect the ratio between intramolecular halogen and intermolecular vibrations in the lowest vibrational states.

Using the C state as the resonant state corresponds to an incoming photon around 29 470 cm^{-1} (λ = 339 nm) for Cl_2 and 23 740 cm^{-1} (λ = 421 nm) for Br_2 in the gas phase (obtained from the maxima in the *ab initio* absorption spectra, Refs. 35 and 36). Results using the B state for Br_2 would be similar since the B state is also repulsive in the region of maximum Franck Condon overlap, around 20 210 cm^{-1} (λ = 495 nm), with the ground electronic state X. We chose the C state because it has the largest absorption intensity and it is entirely repulsive along Q. Also, the B state absorption spectrum was not determined from the *ab initio* potential for Cl_2 in Ref. 36 because of a much smaller intensity.

As a test, we also computed resonant Raman spectra for the isolated halogen molecules, using existing empirical potentials and comparing with the results obtained using the *ab initio* potentials at their largest q value. For chlorine, the C and X potentials were taken from Burkholder and Blair[38] and from Coxon,[39] respectively. For bromine, we used the potential published by Tellinghuisen[40,41] for the C state and by Focsa *et al.*[42] for the X state.

TABLE I. $^{35}Cl_2$ and $^{79}Br_2$ ground state vibrational energies for the empirical RKR potential (Cl_2, Coxon;[39] Br_2: Focsa *et al.*[42]) and for the *ab initio* surface of Hernandez Lamoneda *et al.*[9] (see text). The zero for energies is the potential energy minimum.

	Cl_2			Br_2	
	Energy (cm^{-1})			Energy (cm^{-1})	
v	Empirical	*Ab initio*	v	Empirical	*Ab initio*
0	279.13	269.28	0	162.38	147.9328
1	833.66	806.23	1	485.53	463.1716
2	1382.65	1340.51	2	806.50	776.2834
3	1925.95	1873.80	3	1125.29	1087.618
4	2463.94	2398.80	4	1441.87	1395.8626
5	2996.52	2909.58	5	1756.24	1702.7770
6	3523.48	3403.51	6	2068.38	2008.5667
7	4044.86	3880.48	7	2378.27	2313.8312
8	4560.80	4341.95	8	2685.91	2619.1535
9	5071.70	4790.68	9	2991.27	2925.3063
10	5578.16	5232.44			
11	6081.34	5678.27			
12	6584.55	6143.41			

C. Bound states

The required 1D and 2D bound states have been calculated in the previous publications.[35,36] The 1D vibrational states were calculated using finite difference integration[43] followed by a Numerov-Cooley integration[44] of the energy-resolved Schrödinger equation. Their energies are collected in Table I. The 2D bound states were determined by diagonalizing the vibrational hamiltonian in a product discrete variable representation (DVR) basis.[45] The corresponding energies are reported in Table II for the sake of completeness. Both the Cl_2 and Br_2 *ab initio* potentials give a lower vibrational frequency compared to the ones obtained from the empirical potentials.

TABLE II. $H_2O\cdots^{35}Cl_2$ and $H_2O\cdots^{79}Br_2$ ground state vibrational energies (in cm^{-1}) from the *ab initio* potential by Hernandez Lamoneda *et al.*,[9] reported from Franklin *et al.*, Ref. 35 for Cl_2 and Ref. 36 for Br_2. The zero for energies is the X_2 potential energy minimum. Due to their frequency difference, the intramolecular dihalogen mode v_Q and the intermolecular one v_q are well separated and easily assigned.

	$H_2O\cdots Cl_2$			$H_2O\cdots Br_2$		
v_q \ v_Q	0	1	v_q \ v_Q	0	1	2
0	−605.24	−78.24	0	−966.263 2(4)	−656.830 0(4)	−349.382 5(4)
1	−509.46		1	−866.111 24(7)	−556.398 69(6)	−248.674 93(5)
2	−420.11		2	−771.270 6(6)	−461.326 3(6)	−153.365(1)
3	−337.01		3	−681.721 8(8)	−371.15(4)	...
4	−260.17		4	−597.432 6(2)	−286.88(4)	...
5	−189.46		5	−518.335(2)	−206.7(2)	...
6	−124.79		6	−444.36(2)	...	...
7	−66.12		7	−375.9(4)	...	...
			8	−312.(3)	...	...
			9	−253.(15)	...	...
			10	−196.(36)	...	...

III. RESULTS

The resonant Raman spectra presented below are constructed from wave packets propagated for 12 fs for Cl_2 and $H_2O\cdots Cl_2$, 30 fs for Br_2 and $H_2O\cdots Br_2$. We have carried out convergence tests of the results. Also, as presented in Ref. 24, the time scale associated with the development of intensity in the vibrational progression of Br_2 is ~1 fs/overtone. Therefore, the spectra for the first two overtones presented are fully converged.

A. Cl_2 and Br_2 resonant Raman spectra

Figure 1 shows the Raman intensities for Cl_2 and Br_2 calculated using Eq. (1) with empirical or *ab initio* interaction potentials. Intensities are decaying smoothly because of the acceleration of the wave packet as it evolves on the dissociative excited state.

In addition to the relative vibrational state intensities, our simulation also gives information on the kinetics of the dihalogen dissociation in the excited electronic state. Figure 2 shows the real part of the Cl_2 Raman wave function after 12 fs propagation in the excited electronic state. A similar figure was obtained for Br_2 after 30 fs propagation. For comparison, the $v = 0$ and $v = 1$ vibrational wave functions of the X electronic state are shown. Since intensities are proportional to the squared overlap of the Raman wave function with the X vibrational wave functions, this figure shows that within 12 fs for Cl_2 (30 fs for Br_2), there is time to access many excited vibrational levels in the X state.

This can also be seen in Figure 3, which plots the modulus of the Raman wave function after 12 fs (30 fs) propagation in the C state for Cl_2 (Br_2), together with the initial ground state. In 12 fs, the maximum of the Cl_2 Raman wave function has moved from 2.025 Å to 2.06 Å and it extends up to 2.19 Å (from the distance at which its modulus is 1/10 of its maximum value). For Br_2, the maximum of the Raman wave function moves from 2.32 Å to 2.40 Å in 30 fs and it extends up to 2.72 Å after this time. As seen in Fig. 1, this is enough to populate up to $v = 12$ for Cl_2 and $v \geq 9$ for Br_2.

B. $H_2O\cdots Cl_2$ resonant Raman spectrum

Figure 4 shows the calculated $H_2O\cdots Cl_2$ Raman intensities after 12 fs in the region of $v = 1$ of Cl_2. These results give an important information: the relative inter- to intramolecular vibrational intensity is about 15%.

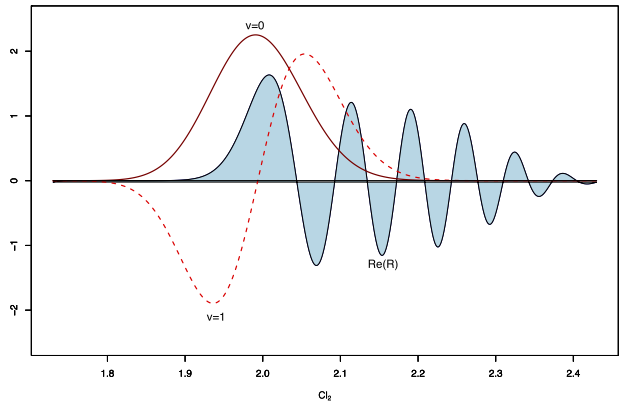

FIG. 2. Real part of the Raman wave function after 12 fs propagation, together with the $v = 0$ and $v = 1$ wave functions of the Cl_2 ground electronic state, showing that the Raman wave function extends way beyond the $v = 1$ wave function. Hence, if the excited electronic state survives for at least 12 fs, there is ample time to populate many vibrational levels in the X state.

This small ratio is due to the fact that in the electronic excited state, dissociation is much faster along the intramolecular coordinate than along the intermolecular one. This is illustrated in Fig. 5, which shows the Raman wave function obtained after 12 fs propagation, together with the initial wave packet. The background shows the potential energy contours in the excited electronic state. Clearly, the slope is larger along the Cl–Cl coordinate than along the water-Cl_2 one.

C. $H_2O\cdots Br_2$ resonant Raman spectrum

In the case of bromine, the results are similar. Fig. 6 shows the calculated Raman intensities after 30 fs propagation in the excited electronic state.

The first intermolecular vibrational level, $v_q = 1$ ($|0,1\rangle$), now amounts to 33% of the intramolecular $v_Q = 1$ ($|1,0\rangle$) intensity (compared to 15% for $H_2O\cdots Cl_2$). This is due to the fact that Br–Br dissociation is slightly slower, and in the excited state potential the difference in slope between the Br–Br coordinate and the water-Br_2 one is smaller than in the case of Cl_2. This can be seen in Fig. 7 which shows the Raman wave function at the end of the excited state propagation,

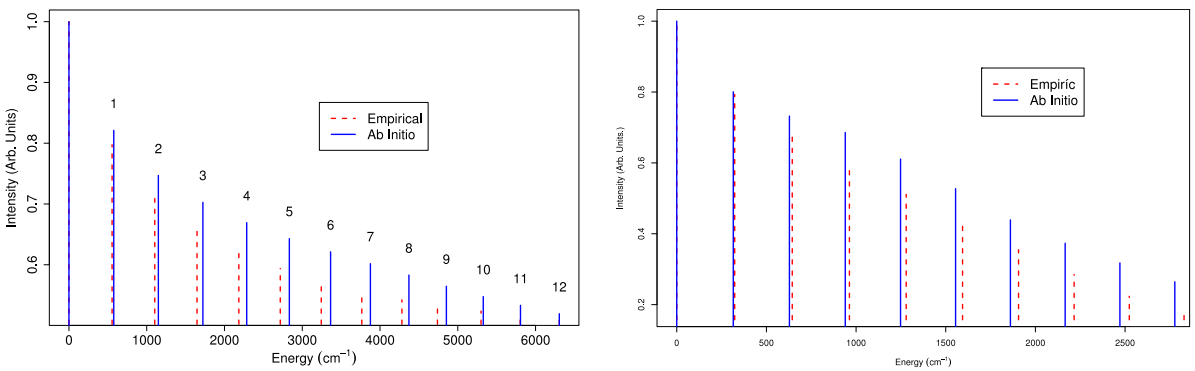

FIG. 1. Calculated Cl_2 (left panel) and Br_2 (right panel) Raman intensities using the empirical (red, dashed lines) or the *ab initio* (blue, straight lines) potentials for the X–X interaction.

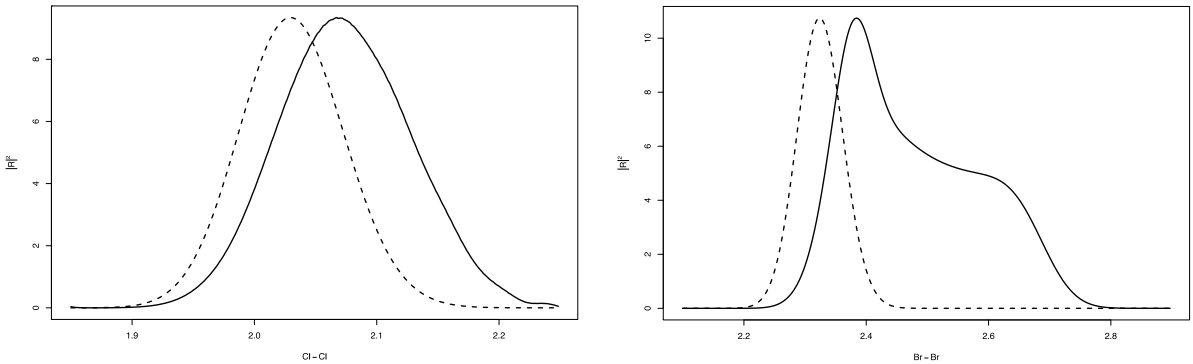

FIG. 3. Modulus of the Raman wave function (solid line) compared to the initial wave function promoted from the ground electronic state (dashed line). Left panel: Cl_2 (propagation time = 12 fs); right panel: Br_2 (propagation time = 30 fs).

compared to the initial wave packet, with the potential energy surface of the excited state in the background.

IV. DISCUSSION

No progression was observed in the resonant Raman study of Br_2 in aqueous solution by Branigan *et al.*[24] This was in contrast with their study using the same technique for liquid Br_2.[25] The absence of a progression was attributed to evolution of the excited state wave packet along many equivalent water-Br_2 coordinates, which reduced the intensity of the Br_2 progression. In the 1:1 complex, there is only one intermolecular coordinate; hence, this effect is not as strong, which in a way makes it easier to see. The propagation along the intermolecular coordinate reduces the intensity of the Br_2 progression and produces a progression for the intermolecular mode. This can be seen by using the same model as in Ref. 24. Let us assume that the wave packet is separable in the excited state and that it is also the case for the bound level wave functions in the ground electronic state. $R(\omega_I)$ [defined in Eq. (2)] can then be written as

$$R(\omega_I) = \phi_e(Q)\psi_e(q) \tag{4}$$

and the wave function of the final vibrational level $v_f \equiv (v_Q, v_q)$ as

$$\langle Qq|g, v_f\rangle = \phi_{g v_Q}(Q)\,\psi_{g v_q}(q). \tag{5}$$

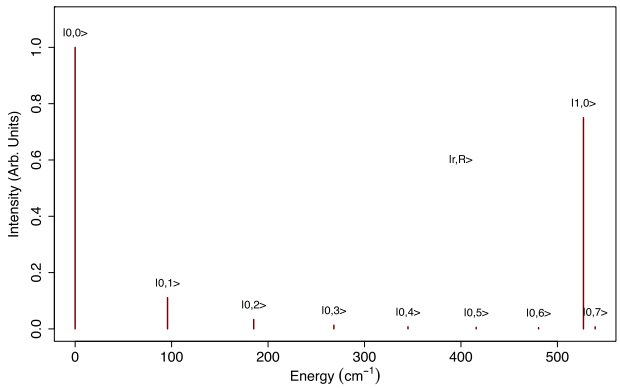

FIG. 4. Calculated $H_2O\cdots Cl_2$ resonant Raman intensities after 12 fs propagation in the $C(^1\Pi_{1u})$ excited electronic state. The lines are labelled as $|v_Q, v_q\rangle$ with v_Q for the dihalogen and v_q for the intermolecular mode.

Reporting these forms in Eq. (1), the Raman intensity is then

$$I_{f\leftarrow i}(\omega_I, \omega_S) \propto |\alpha_{f\leftarrow i}(\omega_I)|^2$$

with

$$\alpha_{f\leftarrow i}(\omega_I) = \left\langle \phi_{g v_Q}(Q)\psi_{g v_q}(q) \mid \phi_e(Q)\psi_e(q)\right\rangle, \tag{6}$$

which can be rewritten as

$$\alpha_{f\leftarrow i}(\omega_I) = \left\langle \phi_{g v_Q}(Q) \mid \phi_e(Q)\right\rangle \left\langle \psi_{g v_q}(q) \mid \psi_e(q)\right\rangle. \tag{7}$$

In the resonant Raman spectrum of isolated bromine, only the first term of the right hand side is present. The second term dispatches the intensity of the dihalogen among different vibrational combinations (v_Q, v_q). This intensity redistribution depends on the motion of the excited wave packet along the intermolecular coordinate, and hence it is a measure of the dynamics in the excited state. If the dihalogen dissociation is so fast that the intermolecular coordinate does not have time to move ("spectator" approximation), then the resonant Raman spectrum of $H_2O\cdots X_2$ is the same as the one for the isolated dihalogen molecule (assuming that the transition dipole moment is mostly carried by the dihalogen coordinate). In the case of $H_2O\cdots Cl_2$, the wave packet moves mostly along the Cl–Cl coordinate, and much less along the intermolecular coordinate, as can be seen from Fig. 5. As a result, the relative inter to intra-molecular intensity (ratio of the $|0,1\rangle$ to $|1,0\rangle$ peaks in Fig. 4) is about 15%. In the case of $H_2O\cdots Br_2$, the wave packet moves a little more along the intermolecular coordinate (Fig. 7), and the resulting ratio of the $|0,1\rangle$ to $|1,0\rangle$ peaks in Fig. 6 is about 33%. This confirms the model presented in Ref. 24 for interpreting the absence of a resonant Raman progression in aqueous solution of bromine. The evolution of the wave packet along bromine-solvent coordinates reduced the bromine progression intensity so much that it was no longer visible. On the other hand, no progression was observed at low frequencies, which would correspond to bath modes, which was interpreted as the absence of the $H_2O\cdots Br_2$ complex as a persistent structure in the solution.

Results over the $B(^3\Pi_{0^+u}) \leftarrow X(^1\Sigma_g)$ resonant transition would have been similar since the B state is also repulsive in the Franck-Condon region, with a slope almost parallel to that of the C states as revealed by the very similar width of the absorption spectrum.[36] Therefore, it is expected that the intermolecular vibration would also be present in

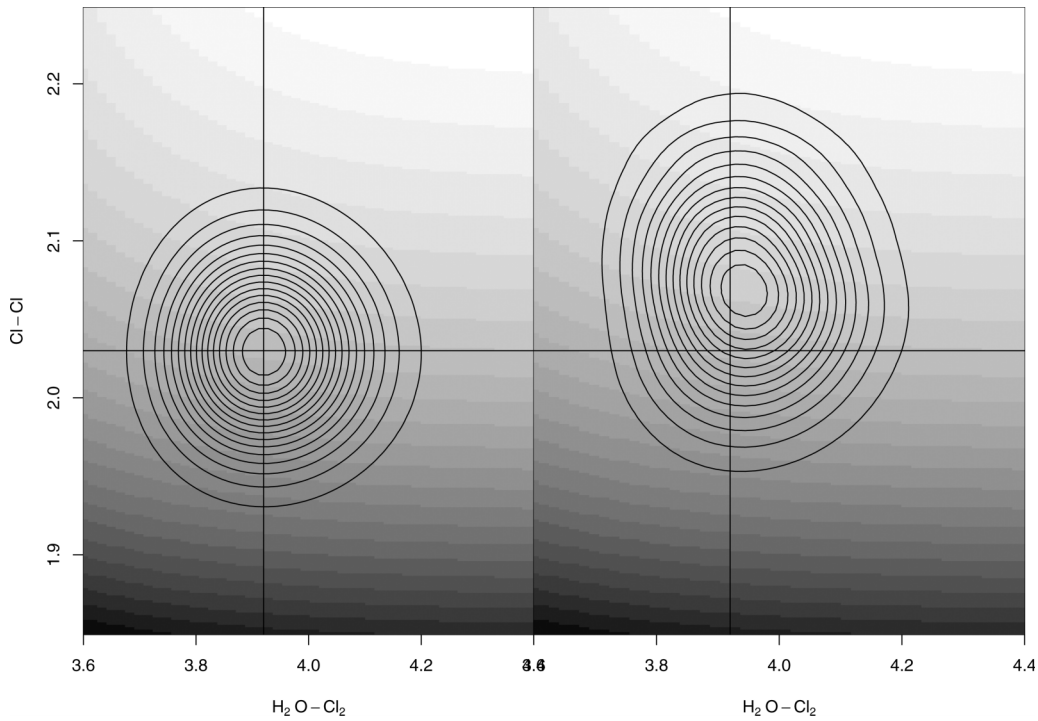

FIG. 5. $H_2O\cdots Cl_2$ initial wave function (left) and modulus of the Raman wave function after 12 fs propagation in the $C(^1\Pi_{1u})$ excited electronic state (right). The background shows the C state equipotentials.

resonant Raman spectra of $H_2O\cdots Br_2$ over the $B(^3\Pi_{0^+u}) \leftarrow X(^1\Sigma_g)$ resonant transition, with a similar intensity ratio to the fundamental compared to the $C(^1\Pi_{1u}) \leftarrow X(^1\Sigma_g)$ resonant transition studied in this work.

A consequence of the existence of low frequency lines corresponding to intermolecular vibrations is that resonant Raman should provide a test for the presence of halogen-bonded complexes. Thus, it could help solve for contradictory experimental results.

It was proposed by Udachin *et al.* that halogen bonds existed in clathrates due to Bjerrum defects in which one of the water molecules of the hydrogen-bonded network forming the cage walls rotates, and can therefore allow one of its lone pair electrons to interact with the host. If this is true, intermolecular vibrations should be detectable in the resonant Raman spectra. One indication that it may be so is the fact

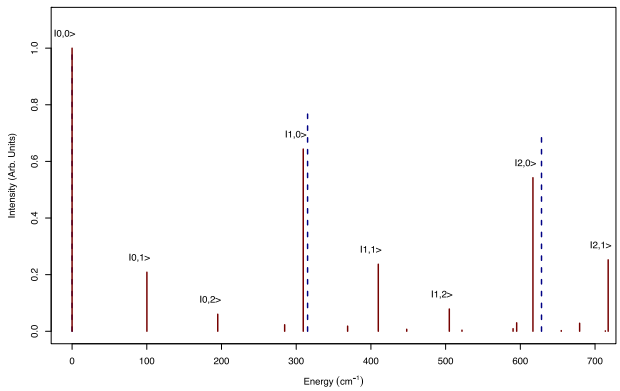

FIG. 6. $H_2O\cdots Br_2$ calculated Raman intensities after 30 fs propagation in the $C(^1\Pi_{1u})$ excited electronic state. The lines are labelled as $|v_Q, v_q\rangle$ with v_Q for the dihalogen and v_q for the intermolecular mode.

that in the T $5^{12}6^2$ cages, bromine molecules point towards one oxygen atom (one of the hexagonal face corners) with a Br–O intermolecular distance (2.91 Å) significantly shorter than the sum of the van der Waals radii (3.37 Å).

In their resonant Raman study of Br_2 clathrates, Goldschleger *et al.*[4] did not mention any low frequency band. There could be weak resonances corresponding to intermolecular water-halogen vibrations hidden in the residual scattering background after subtraction of the intramolecular progression. However, their intensity would be clearly lower than the one predicted here. This points to the absence of $H_2O\cdots Br_2$ complexes in their experiments. The low frequency bands observed by Anthonsen[17] are probably due to lattice vibrations, since they do not show up in the resonant Raman spectra. This seems to indicate that no halogen $H_2O\cdots Br_2$ bond is formed. It should be noted that the RR spectra were carried out at a much higher temperature (−10 °C or 263 K) than the X ray diffraction experiments by Udachin *et al.* (173 K). It could be that at lower temperature, defects are trapped in which bromine molecules relax to a minimum energy site close to the oxygen atom of a water molecule. This could be the equivalent of the stabilization of Bjerrum defects or vacancy defects by H-bonding to guest molecules.[7,8] Since there are several equivalent of these sites, and since translational motion of bromine in the clathrate cage should be low frequency, at higher temperature several translational levels can be populated and Br_2 molecules can appear to be near the cage center. This would be similar to the conclusion reached in the absorption spectrum of Cl_2 in clathrates,[5] where the 500 cm^{-1} additional shift at 77 K was attributed to the sticking of the Cl_2 molecule to the cage wall at low temperature. However, in the X ray experiment, the authors observed librational shortening of Br_2 which was

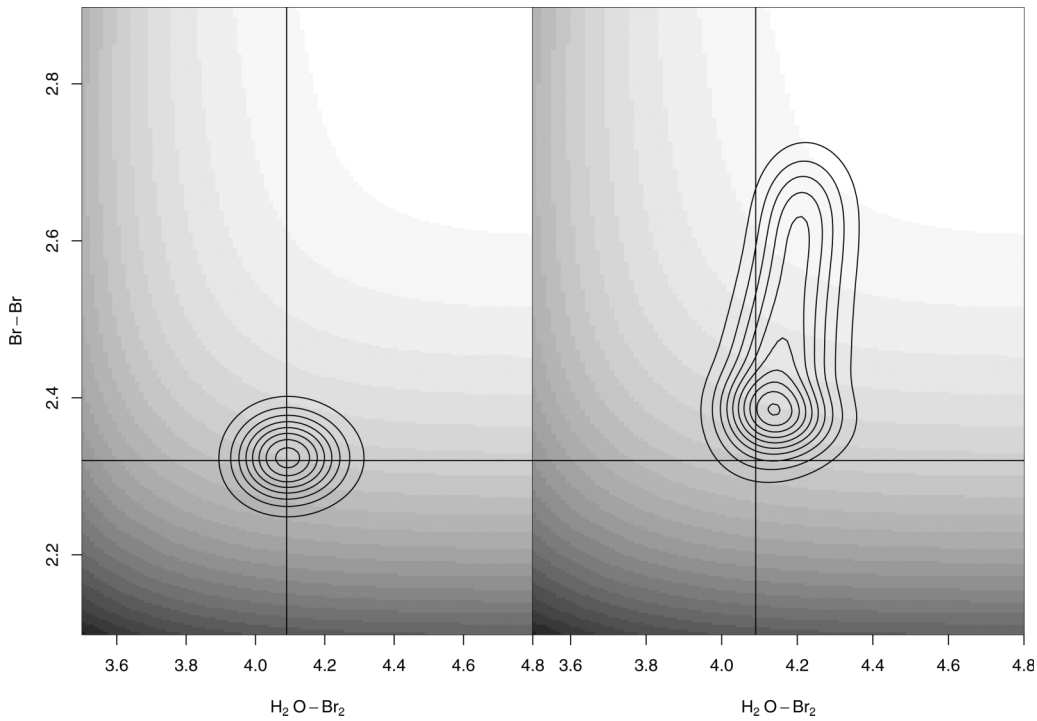

FIG. 7. $H_2O\cdots Br_2$ initial wave function (left) and modulus of the Raman wave function after 12 fs propagation in the $C(^1\Pi_{1u})$ excited electronic state (right). The background shows the *C* state equipotentials.

evidence for their motion in the cage, whereas in the resonant Raman experiment, no additional width due to a rotational envelope was observed, which showed that Br_2 rotation was quenched.

A systematic study of the RR spectra of Cl_2 and Br_2 clathrates as a function of temperature would shed light on the nature of the binding sites of these molecules. In particular, the equivalent of the nonclassical structures observed at low temperatures by Monreal *et al.*[8,46] could be observed in chlorine clathrates, although this is hypothetical at this stage. In these structures, large-cage guests accepted a proton and small-cage guests donated a proton to a common water molecule of the shared wall. Chlorine molecules can sit in both small and large cages, and they could play the role of both the proton acceptor and proton donor. They could act as the equivalent of a proton donor by accepting the lone electron pair orbital of a water oxygen in the large cages. Their role as proton acceptors in the smaller cages is less obvious since the interaction between halogen molecules and the water hydrogens is much weaker, although still significantly stronger than van der Waals interactions.[16] This would explain the sudden appearance of a large shift in the absorption spectrum of chlorine hydrates at low temperature.

Distortions in the water lattice could also play a role in the differences observed between experiments. In a fixed $5^{12}6^2$ cage, *ab initio* calculations[28] give a minimum energy configuration with one bromine pointing to a pentagonal face and the other to the center of an edge between two pentagonal faces. This is not in agreement with the X ray result. Hence, the $5^{12}6^2$ cage containing Br_2 could be distorted, and the distortion could depend on temperature. Also, one bromine atom could be close to an oxygen atom without formation of a halogen bond. Indeed, the electronic density around an oxygen atom involved in the clathrate structure is non-spherical, it is rather close to tetrahedral. The same is true for the halogen atom in the diatomic molecule, in which electronic density is lower outward along the diatomic axis because of the hole in the σ^* orbital. This can give angles along which contact distance can be somewhat smaller than predicted by the sum of van der Waals radii.

Finally, our conclusion that the low frequency intermolecular vibration should be detected if a halogen bond is formed was based on a 2-D model. Including all dimensions in the simulation could, in principle, alter this conclusion. However, it would mean that the wave packet in the excited state would propagate along these additional dimensions. This is rather unlikely, given that the intra- and intermolecular distances are the most strongly coupled coordinates by far. This was the basis for our choice of the 2-dimension model. Therefore, this conclusion should be robust.

V. CONCLUSION

We have determined the resonant Raman spectrum of the halogen bonded $H_2O\cdots Cl_2$ and $H_2O\cdots Br_2$ complexes over the $C(^1\Pi_{1u}) \leftarrow X(^1\Sigma_g)$ transition. Results using the $B(^3\Pi_{0^+u}) \leftarrow X(^1\Sigma_g)$ resonant transition would have been similar. In addition to the vibrational progression in the dihalogen mode, the spectra exhibit a vibrational progression in the intermolecular mode, with relative intensity of about 15% for $H_2O\cdots Cl_2$ and 33% for $H_2O\cdots Br_2$. This should make the $H_2O\cdots Br_2$ halogen bonded complexes detectable in any condensed phase environment where a vibrational progression can be observed for Br_2. This includes the clathrate environment for which experimental results using different techniques lead to contradictory results. Therefore, it

would be worth conducting new resonant Raman experiment in the same experimental conditions as the X ray diffraction spectra, in order to get direct information on the vibrations of the halogen molecules that seem to be oxygen-bonded. For these molecules, the linearity condition for halogen bonding is not fulfilled; hence, it would be interesting to investigate the nature of their bonding in the cage.

In their RR study of aqueous solution, Branigan *et al.* observed no intermolecular lines. Given that Raman probes ephemeral structures that may last for only a few femtoseconds, and given the strength of the intermolecular lines that we predict in the 1:1 complex, the absence of any such signature in the published spectra suggests the absence of distinct halogen-bonded water molecules.

This simulation was conducted in the framework of a 2-dimensional model. The inter to intramolecular intensity ratio should not be significantly affected by taking all degrees of freedom into account since the intramolecular mode is the one carrying most of the oscillator strength and the intermolecular stretching mode is the one most strongly coupled to it.

ACKNOWLEDGMENTS

V.A.A. is supported through the NSF Center for Chemical Innovation on Chemistry at the Space-Time Limit (Grant No. CHE-0802913). The French Embassy in Cuba is gratefully acknowledged for funding extensive stays of R.F.M. in Toulouse.

[1]I. U. Goldschleger, V. Senekerimyan, M. S. Krage, H. Seferyan, K. C. Janda, and V. A. Apkarian, J. Chem. Phys. **124**, 204507 (2006).
[2]G. Kerenskaya, I. U. Goldschleger, V. A. Apkarian, and K. C. Janda, J. Phys. Chem. A **110**, 13792 (2006).
[3]G. Kerenskaya, I. U. Goldschleger, V. A. Apkarian, E. Fleischer, and K. C. Janda, J. Phys. Chem. A **111**, 10969 (2007).
[4]I. U. Goldschleger, G. Kerenskaya, K. C. Janda, and V. A. Apkarian, J. Phys. Chem. A **112**, 787 (2008).
[5]K. C. Janda, G. Kerenskaya, I. U. Goldschleger, V. A. Apkarian, and E. B. Fleischer, "UV-visible and resonance Raman spectroscopy of halogen molecules in clathrate-hydrates," in *Proceedings of the 6th International Conference on Gas Hydrates (ICGH 2008), Vancouver, BC, Canada, 6–10 July 2008* (The University of British Columbia, 2008).
[6]I. U. Goldschleger, G. Kerenskaya, V. Senekerimyan, K. C. Janda, and V. A. Apkarian, Phys. Chem. Chem. Phys. **10**, 7226 (2008).
[7]V. Buch, J. P. Devlin, I. A. Monreal, B. Jagoda-Cwiklik, N. Uras-Aytemizc, and L. Cwiklikb, Phys. Chem. Chem. Phys. **11**, 10245–10265 (2009).
[8]I. A. Monreal, L. Cwiklik, B. Jagoda-Cwiklik, and J. P. Devlin, J. Phys. Chem. Lett. **1**, 290 (2010).
[9]R. Hernández Lamoneda, V. H. Uc Rosas, M. I. Bernal Uruchurtu, N. Halberstadt, and K. C. Janda, J. Phys. Chem. A **112**, 89 (2008).
[10]J. B. Davey, A. C. Legon, and J. M. A. Thumwood, J. Chem. Phys. **114**, 6190 (2001).
[11]A. C. Legon, J. M. Thumwood, and E. R. Waclawik, Chem. - Eur. J. **8**, 940 (2002).
[12]A. Engdahl and B. Nelander, J. Chem. Phys. **84**, 1981 (1986).
[13]K. Johnsson, A. Engdahl, P. Ouis, and B. Nelander, J. Phys. Chem. **96**, 5778 (1992).
[14]F. Ramondo, J. R. Sodeau, T. B. Roddis, and N. A. Williams, Phys. Chem. Chem. Phys. **2**, 2309 (2000).
[15]A. K. Pathak, T. Mukherjee, and D. K. Maity, J. Phys. Chem. A **112**, 744 (2008).
[16]M. I. Bernal-Uruchurtu, G. Kerenskaya, and K. C. Janda, Int. Rev. Phys. Chem. **28**, 223 (2009).
[17]J. W. Anthonsen, Acta Chem. Scand. **29A**, 175 (1975).
[18]K. A. Udachin, G. D. Enright, C. I. Ratcliffe, and J. A. Ripmeester, J. Am. Chem. Soc. **119**, 11481 (1997).
[19]F. Fleyfel and J. P. Devlin, J. Phys. Chem. **92**, 631 (1988).
[20]V. A. Apkarian and N. Schwentner, Chem. Rev. **99**, 1481 (1999).
[21]V. Senekerimyan, I. Goldschleger, and V. A. Apkarian, J. Chem. Phys. **127**, 214511 (2007).
[22]I. U. Golschlegger, M. N. van Staveren, and V. A. Apkarian, J. Chem. Phys. **139**, 34201 (2013).
[23]D. G. Imre, J. L. Kinsey, A. Sinha, and J. Krenos, J. Phys. Chem. **88**, 3954 (1984).
[24]E. T. Branigan, N. Halberstadt, and V. A. Apkarian, J. Chem. Phys. **134**, 174503 (2011).
[25]E. T. Branigan, M. N. van Staveren, and V. A. Apkarian, J. Chem. Phys. **132**, 044503 (2010).
[26]D. P. Schofield and K. D. Jordan, J. Phys. Chem. A **111**, 7690 (2007).
[27]D. P. Schofield and K. D. Jordan, J. Phys. Chem. A **113**, 7431 (2009).
[28]F. A. Batista-Romero, P. Pajón-Suárez, M. I. Bernal-Uruchurtu, and R. Hernández-Lamoneda, J. Chem. Phys. **143**, 094305 (2015).
[29]K. A. Udachin, S. Alavi, and J. A. Ripmeester, J. Phys. Chem. C **117**, 14176 (2013).
[30]S.-Y. Lee and E. J. Heller, J. Chem. Phys. **71**, 4777 (1979).
[31]E. J. Heller, R. L. Sundberg, and D. Tannor, J. Phys. Chem. **86**, 1822 (1982).
[32]S. O. Williams and D. G. Imre, J. Phys. Chem. **92**, 3363 (1988).
[33]D. J. Tannor, *Introduction to Quantum Mechanics: A Time-Dependent Perspective* (University Science Books, Sausalito, CA, 2007).
[34]D. A. Long, *The Raman Effect: A Unified Treatment of the Theory of Raman Scattering by Molecules* (John Wiley and Sons Ltd., 2002).
[35]R. Franklin-Mergarejo, J. Rubayo-Soneira, N. Halberstadt, T. Ayed, M. Bernal Uruchurtu, R. Hernández-Lamoneda, and K. C. Janda, J. Phys. Chem. A **113**, 7563 (2009).
[36]R. Franklin-Mergarejo, J. Rubayo-Soneira, N. Halberstadt, T. Ayed, M. Bernal Uruchurtu, R. Hernández-Lamoneda, and K. C. Janda, J. Phys. Chem. A **115**, 5983 (2011).
[37]W. H. Press, B. P. Flannery, S. A. Teukolsky, and W. T. Vetterling, *Numerical Recipes in Fortran: The Art of Scientific Computing* (Cambridge University Press, 1986, 1992).
[38]J. B. Burkholder and E. J. Bair, J. Phys. Chem. **87**, 1859 (1983).
[39]J. A. Coxon, J. Mol. Spectrosc. **82**, 264 (1980).
[40]J. Tellinghuisen, J. Chem. Phys. **115**, 10417 (2001).
[41]J. Tellinghuisen, J. Chem. Phys. **118**, 1573 (2003).
[42]C. Focsa, H. Li, and P. F. Bernath, J. Mol. Spectrosc. **200**, 104 (2000).
[43]D. G. Truhlar, J. Comput. Phys. **10**, 123 (1972).
[44]J. W. Cooley, Math. Comput. **15**, 363 (1961).
[45]J. V. Lill, G. A. Parker, and J. C. Light, Chem. Phys. Lett. **89**, 483 (1982).
[46]I. A. Monreal, J. P. Devlin, Z. Maşlakcı, M. B. Çiçek, and N. Uras-Aytemiz, J. Phys. Chem. A **115**, 5822 (2011).